Proceedings of ASME FEDSM'02
ASME 2002 Fluids Engineering Division Summer Meeting
Montreal, Quebec, Canada, July 14-18, 2002

FEDSM2002-31449

COUPLED THERMAL AND MECHANICAL EFFECTS IN INJECTED POLYMER PIECES: COMPARISON BETWEEN EXPERIMENTAL MEASUREMENTS AND NUMERICAL PREDICTION OF BOTH PRESSURE AND THERMAL CONTACT RESISTANCES TIME EVOLUTION

Hugues MASSÉ, Éric ARQUIS
Laboratoire Master, Ecole Nat. Sup. de Chimie et de Physique de Bordeaux, 16, av. Pey Berland, 33607 Pessac Cedex, France
masse@lmaster.u-bordeaux.fr
arquis@lmaster.u-bordeaux.fr
tel: +33 5 56 84 66 67
fax: +33 5 56 84 66 68

Didier DELAUNAY
Laboratoire de Thermocinétique, Ecole Polytechnique Universitaire de Nantes, CP 3023, 44087 Nantes Cedex 03, France

delaunay@isitem.univ-nantes.fr
tel: +33 2 40 68 31 42
fax: +33 2 40 68 31 41

ABSTRACT

During the cooling of an injected polymer, a very strong coupling exists between the thermal and mechanical phenomena. In order to fill in the mold and to compensate the effects of reduction of the thermal shrinkage, the pressure in the molding cavity is maintained to a very high level. The purpose of this paper is to show the essential importance of thermomechanical coupling present during the cooling of a hot polymer in a cold mold via a comparison between experiments and numerical simulation.

Experiments show that the polymer-mold contact evolves under the effect of the internal contraction caused by the lowering of temperature. On the one hand, the air gap width, depending on the shape of the part, modifies the Thermal Contact Resistance (TCR) between the mold and the part. On the other hand, shrinkage is divided between the two sides of the part depending on the internal stresses, so that the geometry of the part is also linked to changing temperature.

The resolution of the coupled thermal and mechanical problems allows us to predict the shape of the part, the stresses, the temperature field in the polymer and in the surrounding mold, and the air gap widths on both sides.

INTRODUCTION

This paper presents the results of a study permitting to determine the polymer-mold contact resistances in the process of injection molding of thermoplastics. They are related to the pressure and the roughness of the mold. A simulation is done to take into account the thermomechanical coupling and the results are compared to the experience.

During the cooling of an injected polymer, a very strong coupling exists between the thermal and mechanical phenomena. Indeed, the decrease of the temperature provokes a shrinkage that, when the gate is frozen leads to the decrease of the pressure. It provokes a strong modification of the polymer-mold contact conditions, capable to provoke the apparition of an air gap. The pressure conditions the cooling therefore. When the piece is no more in contact with the mold, its shape, therefore the local thickness of the air gap is determined by its movements and therefore the field of stresses in the piece. One conceives the very strong triangular coupling existing between the temperature, the conditions of interface and the pressure (or the stresses in the solid).

We firstly present the results of a study permitting, for an amorphous material, to link the evolution of the contact resistance between the polymer and the mold to the one of the pressure in the molding cavity. The modelling and the simulation of the coupling between thermal and mechanical phenomenon during the cooling of the piece are presented. A characteristic experience of molding of ABS is simulated and the results of measured and calculated temperature and pressure evolutions in the molding cavity are compared.

NOMENCLATURE

Cp	*specific heat* ($J.kg^{-1}.K^{-1}$)
E	*Young's modulus* (Pa)
k	*thermal conductivity* ($W.m^{-1}.K^{-1}$)
K	*bulk modulus* (Pa)
p	*pressure* (Pa)
R	*thermal resistance* ($m^2.K.W^{-1}$)
TCR	*thermal Contact Resistance* ($m^2.K.W^{-1}$)
T	*temperature* (K)
t	*time* (s)
U	*displacement vector* (m)
v	*specific volume* ($m^3.kg^{-1}$)

Greek symbols

α	*linear thermal expansion coefficient* (K^{-1})

β	*volumetric thermal expansion coefficient (K^{-1})*
δ	*air gap thickness (m)*
$\overline{\overline{\varepsilon}}$	*strain tensor (-)*
λ	*1st Lamé coefficient (Pa)*
μ	*2nd Lamé coefficient (Pa)*
ν	*Poisson's coefficient (-)*
ρ	*density ($kg.m^{-3}$)*
$\overline{\overline{\sigma}}$	*stress tensor (Pa)*
τ	*temperature variation (K)*

subscripts and superscripts

air	*relative to air*
0	*initial*
*	*relative to the interface*
g	*relative to the glass transition*

1. GENERAL PRESENTATION

The thermal transfer at the interface between the part and the mold wall is closely linked to the quality of the contact between steel and polymer. S. Quilliet showed the influence of the pressure on the thermal kinetics: the higher the pressure, the better the contact; so the thermal transfer is thus improved and the part cools quicker. Moreover, the part can become unstuck from the wall, which has a strong influence on the thermal behaviour. So one sees that precise knowledge of the thermal evolution requires the correct determining of pressures and displacements, which then allows to evaluate the quality of the contact or to calculate thicknesses of the air gaps.

The simulation uses the finite volumes method. Traditionally, the equations of the solid mechanics are solved by finite elements methods. Some authors begin however to use the finite volumes to solve these equations in particular I. Demirdzic [1, 2]. Hattel [3] uses also a technique of finite differences.

One applies the small perturbation hypothesis (small displacements, small strains, small temperature variations), that supposes that the displacements between two time steps in the solid material are sufficiently small. The position of the nodes of the mesh remains unaltered during the calculation, but a displacement of these nodes is calculated during time.

2. FORMULATION OF THE EQUATIONS

In order to take into account the thermo-mechanical coupling phenomena that occur during the injection molding, it is necessary to simultaneously solve the equations governing the temperature evolution, the mechanical deformations and the PVT variations of the material.

We use an amorphous polymer (ABS) whose thermal conductivity, specific heat and PVT diagram are precisely characterised by our measurements.

a. State equation:

The specific volume links the variations of temperature and pressure to the volume of the material through the PVT diagram. This relation designed as state equation may be written in the general form:

$$f(P,v,T)=0 \tag{1}$$

Although theoretical approaches of this state equation exist, it is generally represented by an empirical model based on the measurements. We chose the well known Tait relation [4] which gives a good approximation of the PVT diagram and whose coefficients have been tabulated for many polymers. This relation is :

$$\frac{\upsilon(0,\widetilde{T})-\upsilon(p,\widetilde{T})}{\upsilon(0,\widetilde{T})}=C\ln\left(1+\frac{p}{B(\widetilde{T})}\right) \tag{2}$$

with $\widetilde{T}=T-\left[T_g(p)-T_g(0)\right]$

The variation of T_g =f(p) is linear, its evolution is deduced from experimental results

$$T_g(p)=T_g(0)+\frac{0.55}{3}p \tag{3}$$

One notes that the use of this relation requires the knowledge of three parameters :

- the specific volume at atmospheric pressure $\nu(0,T)$,
- The adimentional constant C,
- The function B(T), that has the dimension of a pressure.

Simha and al. [5] showed that C is nearly constant (best approximation : C=0.0894) and that B(T) can be written:

$$B(T)=b_1e^{-b_2T} \tag{4}$$

The constant b_2 has a mean value of $4.5.10^{-3}$ while b_1 depends on the nature of the polymer, but is proportional to the elastic module of compression $K=\frac{E}{3(1-2\nu)}$. We use $b_1=3.3.10^{-2}$ K, which permits to approach the measurements satisfactorily (Fig. 1b).

The knowledge of the PVT diagram of the material permits to deduce the values of the density and of thermal expansion coefficient, which depend at a time on the temperature and the pressure:

$$\rho=\frac{1}{v};\ \alpha=\frac{1}{v}\left(\frac{\partial v}{\partial T}\right)_p;\ \beta=\frac{\alpha E}{1-2\nu} \tag{5}$$

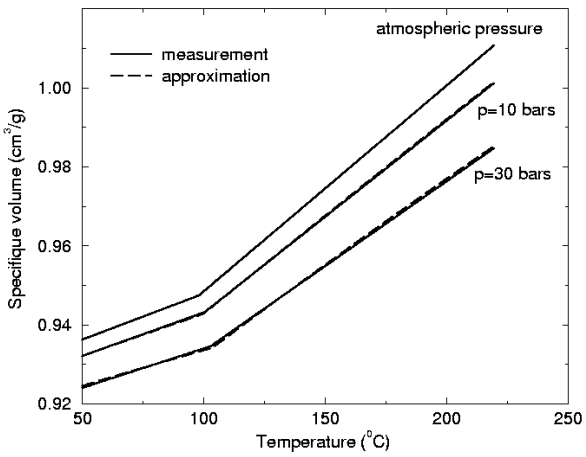

Figure 1: PVT diagram

The use of this last equation includes some limitations however. Indeed, even though it is possible to give a realistic enough evolution of the Poisson's coefficient (for example ν=0.2 for T < Tg and ν=0.4 for T>Tg), the detachment of the piece makes the bulk modulus unrealistic when the pressure at the surface of the piece becomes equal to the atmospheric one. It is then necessary to use the measured values of the Young modulus.

b. displacements equation:

In the formulation that we propose, the equilibrium equation is written and allows to obtain the discrete displacements equation (on an irregular Cartesian mesh) following the way presented on Fig. 8.

$$\nabla.\overline{\overline{\sigma}} = 0 \tag{6}$$

The elastic behavior leads to write the stress tensor:

$$\overline{\overline{\sigma}} = \lambda\left(tr\,\overline{\overline{\varepsilon}}\right)\overline{\overline{I}} + 2\mu\,\overline{\overline{\varepsilon}} - \beta\tau\overline{\overline{I}} \tag{7}$$

The equation that links the deformation to the displacements is then used:

$$\overline{\overline{\varepsilon}} = \frac{1}{2}\left(\nabla U + \nabla^T U\right) \tag{8}$$

We get then the displacements (or Navier) equation:

$$\nabla\left(\lambda\nabla.U\right) + \nabla.\left[\mu\left(\nabla U + \nabla U^T\right)\right] - \nabla\left(\beta\tau\right) = 0 \tag{9}$$

After the discretization, we get a matrix system where the main blocks A and D contain five diagonals, while the coupling blocks B and C contain nine diagonals:

$$\begin{bmatrix} A & B \\ C & D \end{bmatrix}\begin{bmatrix} U \\ V \end{bmatrix} = \begin{bmatrix} \phi_x \\ \phi_y \end{bmatrix} \tag{10}$$

c. energy equation:

The equation of the energy is written in the form of:

$$\frac{1}{v}C_p(T)\frac{\partial T}{\partial t} - \alpha(T,p)T\frac{\partial p}{\partial t} = \nabla.\left(k(T)\nabla T\right) \tag{11}$$

Besides the thermal contact resistance due to the imperfect contact between mold and polymer, a thermal resistance exists due to the air gap that can come in between the piece and the mold during the cooling. It is therefore necessary to know the displacements and the deformation of the piece to calculate this thermal resistance correctly.

At the time of the detachment, that is to say when the stress at the polymer-mold interface becomes equal to the atmospheric pressure, an initial thickness of the air gap equal to the value of the contact resistance at this instant is considered. The interface conductance expresses then:

$$h(t) = \frac{1}{\dfrac{\delta}{R_{air}} + R\left(p(t)\right)} \tag{12}$$

Thermal conductivity and specific heat have been measured at the laboratory and have been used in the simulation. The density comes from the PVT diagram and depends therefore on both pressure and temperature.

3. THERMOMECHANICAL COUPLING

When using a global approach, the coupling between the thermal and mechanical fields of the problem must be taken into account. Let us suppose for instance a hot polymer in touch with a cold mold. During its cooling, the polymer part shrinks and eventually become unstuck from the mold walls, which causes an air gap to appear. This acts as thermal insulation and slows down the cooling kinetics. Thermomechanical coupling occurs because the heat transfer is linked to the air gap thickness, which depends itself on the thermal condition of the mold-part system.

In a simple case, time has no influence on the resolution of a thermoelastic problem. The elastic behavior law is not time-dependent: a given stress has an immediate effect. The unsteady thermomechanical problem can thus be solved as a succession of solicitations. This can be illustrated by the following example of a cooling part. Let us take a part whose initial temperature is T_1 cooled on one side at the T_0 temperature, the other sides supposed to be adiabatic ones. Zero

stresses are imposed on all the sides of the part, which can therefore expand or shrink freely.

1. At the time Δt, the temperature field is T_1. The difference in temperatures τ is then $T_1 - T_0$, which corresponds to a $\mathbf{U}_1$ displacement.

2. At the time $n\Delta t$, the temperature field is T_n. The difference in temperatures τ is then $T_n - T_0$, which corresponds to a $\mathbf{U}_n$ displacement.

It can be noticed that the displacements field at the time $n\Delta t$ is totally independent of the mechanical state at the previous times. There is a direct relation between temperature and displacements, with no dependence on time. This is due to the fact that the temperature and displacement fields are not coupled.

In a other hand, if instead of having a side at constant temperature T_0, there is another non-deformable isothermal part initially in contact with the sample, a coupling occurs. Actually, the sample will shrink and so move away from the cold source, causing an air gap to settle in between. The temperature field depends then on the displacements field, as in the previous case, but also on the temperature field itself via the air gap width. There is then a coupling between thermal and mechanical phenomena, which have to be solved at the same time.

The resolution algorithm is written as follows:

1. Thermal characteristics are known at the n^{th} timestep;

2. The thermal calculation gives the temperature field at the $n+1^{th}$ timestep (T_{n+1});

3. The mechanical calculation is done using the temperature field increment $T_{n+1}-T_n$ and gives the partial displacements field $\mathbf{U}^*_{n+1}$;

4. The stresses and strains fields σ^*_{n+1} and ε^*_{n+1} are calculated from $\mathbf{U}^*_{n+1}$;

5. The final fields are calculated with a superposition of the fields at each timestep: $\sigma_{n+1} = \sigma_n + \sigma^\#_{n+1}$, $\varepsilon_{n+1} = \varepsilon_n + \varepsilon^\#_{n+1}$, $\mathbf{U}_{n+1} = \mathbf{U}_n + \mathbf{U}^\#_{n+1}$.

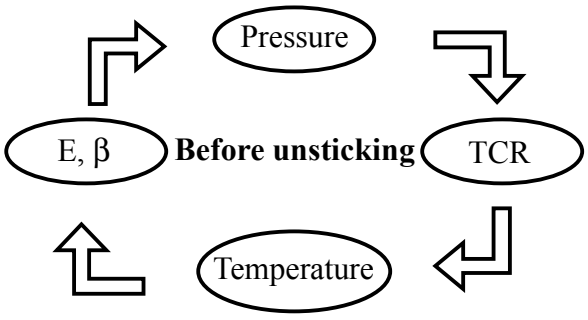

Figure 2-a: coupling before unsticking

6. Once the values of temperature and stresses (or pressures) are established, rheological laws can be used to adjust the thermophysical parameters.

So, in the case of injection molding, the thickness of the air gap, resulting from both the contraction of the part and the former pressure evolution, will modify the TCR. This triangular coupling temperature - interface state - pressure (or stress when the part is solid) therefore appears differently during the cooling, depending on whether the pressure in the cavity is superior or not to the atmospheric pressure (Fig. 2-a and 2-b):

1.The evolution of the pressure in the moulding cavity depends on the temperature field in the polymer through the evolution of the specific volume under pressure (PVT diagram). The temperature field in the part depends itself on the variations of the TCR according to the equation $R=R_0 \exp(-p/p_0)$ (R_0 and p_0 depend on the roughness of the mould).

2. Secondly, when the pressure in the moulding cavity reaches the atmospheric pressure, an air gap appears, whose thickness is the consequence of the PVT diagram. The local distribution of this air gap on each side of the part depends on the distribution of stresses that are created in it. It is therefore impossible to accurately calculate the temperature field without coupling it with the stress field.

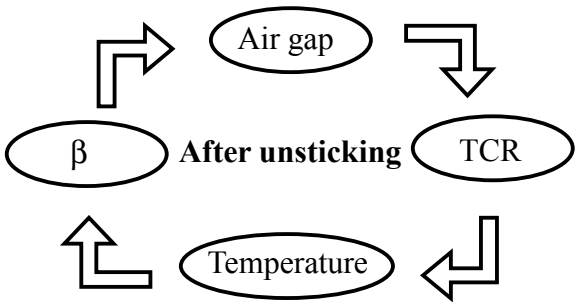

Figure 2-b: coupling after unsticking

The use of the "superposition" principle allows to take into account coupled thermoelastic phenomena. However, the final fields being the sum of all the intermediate fields, it is then necessary to accurately solve the equations at each timestep. This timestep has to be chosen carefully: if it is too large it does not allows the coupling to be properly solved; and if too small it leads to lengthy calculation times.

4. AIR GAP

The knowledge of the TCR alone is insufficient, as an air gap does appear between the walls of the mold and the part. The computation of the field of displacement then makes it possible to determine the thickness of these air gaps.

The presence of an air gap between the piece and the molding cavity is taken into account in the following way:

Concerning the thermal part: the width of the air gap is calculated by the mechanical part for each node of the interface. A thermal conduction model using a three-layer serial

association (half a control volume of steel, the air gap, half a control volume of polymer) is then used to calculate the thermal equivalent conductivity which is used in the thermal model:

$$k^* = \frac{\Delta x}{R_0 + TCR + R_{air}} \quad (13)$$

where R_0 is the thermal resistance for perfect contact, TCR is the expression of the resistance depending on the pressure when there is contact, and $R_{air}=\delta/k_{air}$ where δ is the thickness of the air gap.

This serial model allows all the contributions to the thermal resistance to be taken into account, i.e. pressure, mold roughness and the width of the air pocket.

Concerning the mechanical part: In case there is an unsticking, the interface mesh points gets the "mechanical" properties of air (i.e. E=0). This interface mesh belongs to the mold and therefore has the thermal properties of steel. Its mechanical characteristics are thus variable: steel when there is contact or air when there is no contact, so that the part can move.

5. RESULTS

The parietal flux measurement is delicate, the sensors being generally intrusive. A specific sensors has been designed and is described in the references [6] and [7]. Figure 3 shows a schematic view of this sensor. It is made of the same material and have the same surface roughness than the mold. They allow to determine by inverse method the evolutions of the temperatures and fluxes at the surface of the mold. Their time constant is very small and precise measurements are possible every 5 ms.

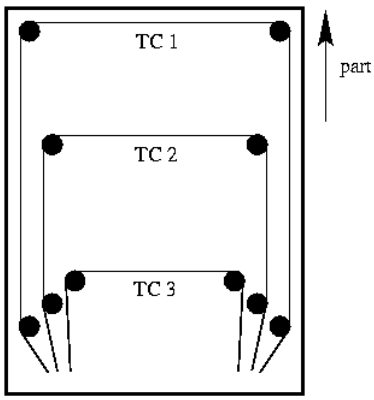

Figure 3: the heat flux sensor is made of three thermocouples

The result we show corresponds to a packing pressure of 2.6 MPa, the temperature mold regulation being programmed in order to ensure a thermal disymmetry through the part. This mold permits to achieve square pieces of 2 mm thickness. The flux sensors are arranged on the two large faces of the part.

Figure 4 shows the evolution of temperatures during an injection cycle. The three values of temperatures measured by each of the thermocouples constituting the sensor are shown. The polymer surface temperature evolution has been obtained by an inverse method described in the reference [8].

One notes the instant of the ejection, 25 seconds after the injection, the evolution of the surface temperature showing an angular point.

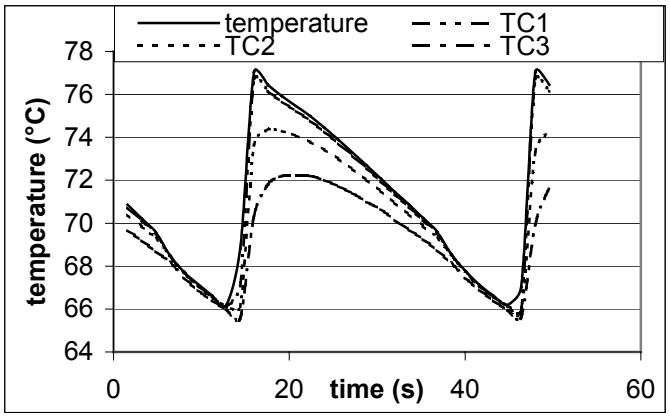

Figure 4: Data given by the flux sensor and identified temperature.

Concerning the numerical simulation, the bi-dimensional calculation domain includes the polymer, the air gaps (when they are present), and the mold. Equations are discretized using a finite volume method on a fixed Cartesian grid and lead to linear systems that are solved using a conjugated gradient method associated with a MILU or Jacobi preconditioning.

The physical parameters depend simultaneously on the temperature and the pressure; the equation of state (1) solved in the polymer is coupled with the two previous equations (9) and (11). They are solved in a totally coupled way, which allows to predict the pressure or the shape of the part, stresses and temperatures in the polymer as well as in the mold.

The computation code has been validated using many benchmarks [9]: the modelling of the TCRs, the ability to take into account the sticking/unsticking on walls or the residual stresses prediction which showed that the code can manage complex situations.

Figure 5 shows the evolution of surface temperatures (respectively on the mold and polymer sides) versus time. One notes the thermal effect of the unsticking that entails a 12°C increase of the polymer temperature. This corresponds to the experimental observations (Fig. 4) [7]. The surface temperature increases then and could reach a value higher than the glass transition one, which would lower the residual stresses trapped in the part.

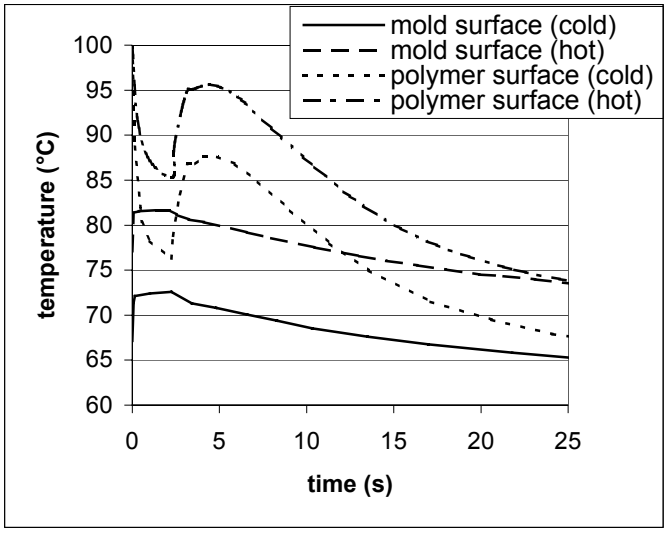

Figure 5: Computed temperatures at the polymer – mold interface.

Figure 6 depicts the evolution of the thermal resistance versus time (in the middle plane of the part). Before the unsticking, the TCR obeys a *TCR*=f(*p*) law built up from experiments [10], therefore having the same value on both faces of the part, because the pressure is uniform throughout it. After the detachment the thermal resistance is due to the air gap that arises between the polymer and the mould. It is noted that these values on the two faces are then different, which is due to the asymmetric cooling.

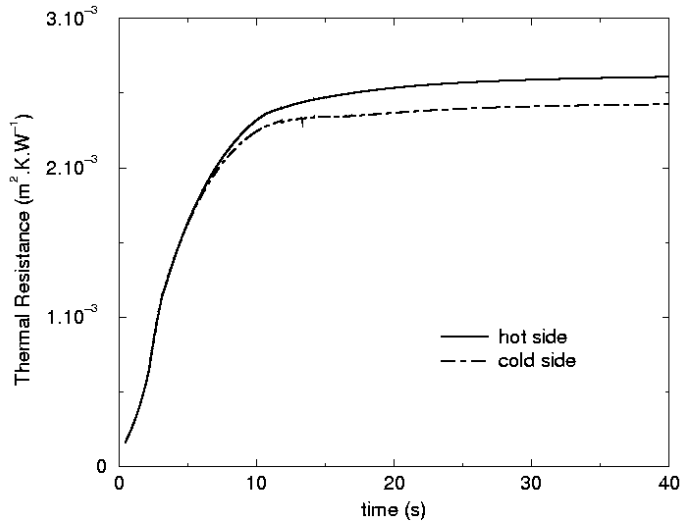

Figure 6: Evolution of the thermal resistance during the cooling of the part.

6. CONCLUSION

The code whose results are presented here is a tool designed to improve the knowledge of the thermomechanical effects that appear during the cooling of a injected piece. We present the results given by our code and we compare them to experimental results. This study presents precise measurements collected by heat flux sensors. The analysis by inverse method permits to extract from the measurements the surface temperatures of the polymer and the thermal resistances. The computation on a 2 mm thickness part allowed us to compare numerical simulation and experiments on a case of simple cooling. The calculation is based on simple hypotheses from a mechanical point of view since it supposes an elastic material whose Young modulus and Poisson's coefficient are temperature dependant. The thermal resistance evaluation taking into account of the coupling between heat transfer and mechanical phenomena, associated to a modelling of the elastic behaviour, permits to calculate with precision the surface temperature evolution. The polymer surface warming-up phenomenon at the time of the unsticking is correctly modelized and its amplitude correlates with the experimental observations.

REFERENCES

[1] I. Demirdžić, D. Martinović, Finite volume method for thermo-elasto-plastic stress analysis, Comput. Methods Appl. Mech. Eng., vol. 109, pp. 331-349, 1993.
[2] I. Demirdžić, S. Muzaferija, Finite volume method for stress analysis in complex domains, Comput. Methods Appl. Mech. Eng., vol. 37, pp. 3751-3766, 1994.
[3] J.H. Hattel; A control volume-based finite difference method for solving the equilibrium equations in terms of displacements, Appl. Math. Modelling, vol. 19, pp. 210-243, 1995.
[4] D.W. Van Krevelen. Properties of polymers. Elsevier, 1990.
[5] R. Simha, P.S.S Wilson, O. Olabisi, Kolloid-Z, vol. 2, pp. 402, 1973.
[6] D.Delaunay, Ph. Le Bot, R. Fulchiron, J.F. Luyé, G. Regnier, "Nature of contact between polymer and mold in injection molding. Part 1: Influence of a non perfect thermal contact, Polymer Engineering and Science, Volume 40, Number 7, July 2000
[7] Ph. Le Bot,"Comportement thermique des semis-cristallins injectés. Application à la prédiction des retraits", Thèse de Doctorat, Université de Nantes, 1998
[8] S.Quilliet, Ph. Le Bot, D.Delaunay, Y. Jarny, "Heat transfer at the polymer-metal interface: a method of analysis and its application to injection molding", ASME Proceedings of the 32nd national heat transfer conference, HTD-Volume 340, volume 2, pp 9-16, 1997
[9] H. Massé, "Couplage thermomécanique lors de la solidification de matériaux polymères", Ph.D. Thesis, Université de Bordeaux 1, 2000
[10] S. Quilliet. Transferts thermiques à l'interface polymère-métal dans le procédé d'injection des thermoplastiques. Ph.D. thesis. Université de Nantes, 1998.